

Chapter 20:
Biomechanical Changes of the Optic Disc

Ian A. Sigal^{1,2}, Michael D. Roberts², Michael J.A. Girard²,
Claude F. Burgoyne³, J. Crawford Downs²

¹Department of Biomedical Engineering,
Tulane University,
New Orleans, Louisiana, USA

²Ocular Biomechanics Laboratory and
³Optic Nerve Head Research Laboratory
Devers Eye Institute
Legacy Health System
Portland, Oregon, USA

Correspondence:
J. Crawford Downs, PhD
Devers Eye Institute
Ocular Biomechanics Laboratory
1225 NE 2nd Avenue
Portland, Oregon, 97232, USA
Phone: 503-413-5320
Fax: 503-413-5179
cdowns@deverseye.org

Clinical Background

1- Ocular biomechanics in glaucoma

Lowering intraocular pressure (IOP) remains the only proven method of preventing the onset and progression of glaucoma, yet the role of IOP in the disease remains controversial. This largely arises from the wide spectrum of individual susceptibility to IOP wherein a significant number of patients with normal IOPs develop glaucoma (e.g. normotensive glaucoma), and other individuals with elevated IOP show no signs of the disease. It is therefore important to understand the relationship between IOP and glaucomatous optic neuropathy when IOP is only one of several factors that influence the disease. IOP is, by definition, a mechanical entity – the force per unit area exerted by the intraocular fluids on the tissues that contain them. Glaucomatous optic neuropathy is a biologic effect – likely the result of an IOP-related cascade of cellular events that culminate in damage to the retinal ganglion cell (RGC) axons. One of the challenges of biomechanics is to understand how the mechanics are transduced into a biological response and/or tissue damage. How does this take place? Why is there such a wide range in susceptibility to IOP? Why does elevated IOP lead to that particular cascade of events and not another? What can we do to predict, detect, and stop the progression of glaucomatous damage? Unfortunately we do not have answers to these questions, but in recent years there has been considerable progress towards understanding of the role of IOP in glaucoma. In this chapter, we focus on two main themes: what is known about how IOP-related forces and deformations are distributed in the posterior pole and ONH, and what is known about the response of the living system.

Pathology

From a biomechanical perspective, the ONH is a natural site of interest when studying IOP effects because it is a discontinuity in the corneo-scleral shell. Such discontinuities are often weak spots in mechanically loaded systems because they give rise to significant stress concentrations¹. In addition, it is the ONH, the lamina cribrosa (LC) in particular, that is the principal site of RGC axonal insult in glaucoma². Nevertheless there is as evidence both for³ and against⁴ direct, IOP-induced damage to the retinal photoreceptors, and it is likely that there are also important pathophysiologies within the lateral geniculate and visual cortex⁵.

Etiology

We have proposed that the ONH be understood as a biomechanical structure, and that the mechanical effects of IOP on the tissues of the ONH, namely forces and deformations, are central determinants of both the physiology and pathophysiology of the ONH tissues and their blood supply at all levels of IOP (**Figure 1**). Within this framework, the susceptibility of a particular patient's ONH to IOP-related insult is a function of the biomechanical response of the constituent tissues and the resulting mechanical, ischemic and cellular events driven by that response. Experienced over a lifetime at physiologic levels of IOP, these events underlie normal ONH aging. Hence, eyes with a particular combination of tissue geometry and stiffness may be susceptible to glaucomatous damage at normal IOP, while others may have a combination of ONH tissue geometry and stiffness that render them impervious to any deleterious effects of high IOP.

We believe that the mechanical and vascular mechanisms of glaucomatous injury are inseparably intertwined: IOP-related mechanics determines the biomechanical

environment within the ONH, mediating blood flow and cellular responses through various pathways. Reciprocally, the biomechanics depend on tissue anatomy and composition, which are subject to change through cellular activities such as remodeling. The interrelationship between mechanics and physiology could be particularly strong within the LC due to its complexity. The LC is composed of a three-dimensional network of beams of connective tissue, many containing capillaries, that provides functional and structural support to the RGC axons. IOP-related forces within the LC could deform the beams containing capillaries, diminishing the blood supply to the laminar segments of the RGC axons. Conversely, primary insufficiency in the blood supply to the laminar region could introduce cell-mediated connective tissue changes that could remodel the extracellular matrix (ECM) making the laminar beams more prone to failure, and limit the diffusion of nutrients to adjacent RGC axons.

Before proceeding with a presentation of the mechanical effects of IOP on the eye and ONH, we review the basic concepts of mechanics relevant to this analysis.

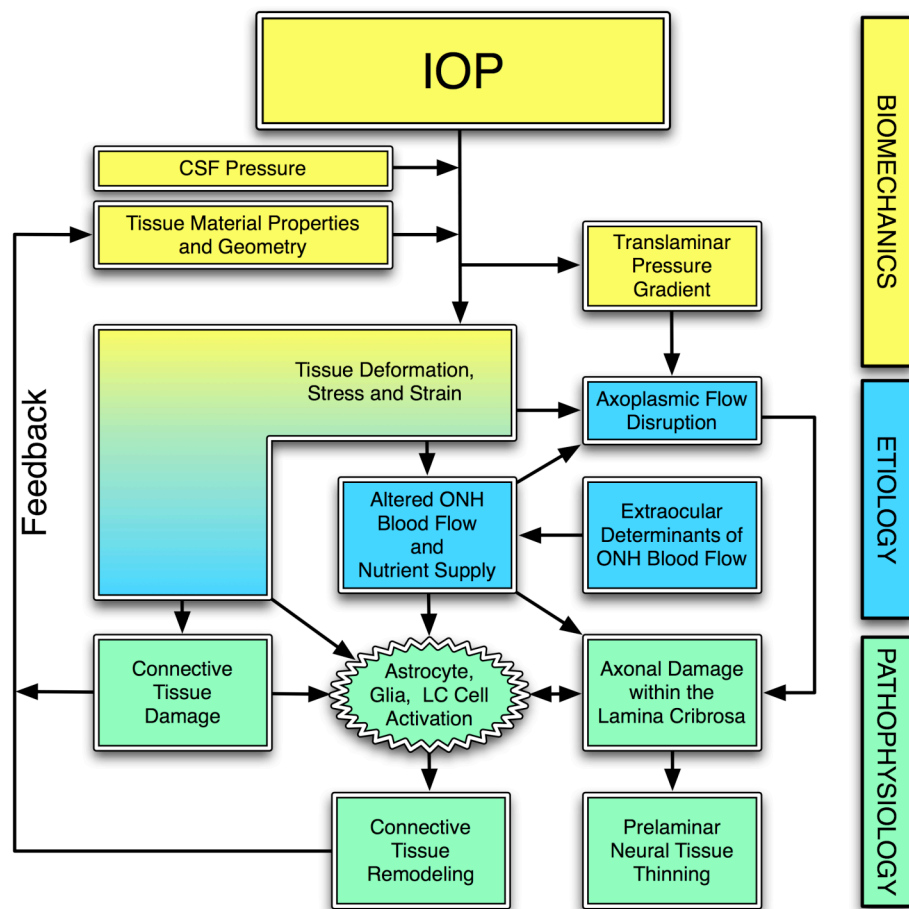


Figure 1. IOP acts mechanically on the tissues of the eye, producing deformations, strain and stress within the tissues. These deformations depend on the particular geometry and material properties of the tissues of an individual eye. In a biomechanical paradigm, the stress and strain will alter the blood flow (primarily), and the delivery of nutrients (secondarily) through chronic alterations in connective tissue stiffness and diffusion properties. IOP-related stress and strain could also induce connective tissue damage directly (LC beam failure), or indirectly (cell mediated), and eventually connective tissue remodeling that alters the geometry and tissue mechanical response to loading. This feeds back directly onto the mechanical effects of IOP, or indirectly by affecting IOP regulation.

2- Basic concepts in mechanics

The following are fundamental terms and concepts from mechanics that may not be familiar to clinicians. The interested reader may pursue these ideas in greater depth by referring to appropriate textbooks ¹.

Stress is a measure of the forces transmitted through, or carried by, a material or tissue. Specifically, stress is the force divided by the cross sectional area over which it acts. For example, pressure is a stress and can be expressed in pounds per square inch (psi).

Strain is a measure of the local deformation induced by an applied stress. It is computed as the change in length of a material divided by its resting length, and is often expressed as a percentage. For example, a wire that was originally 10 mm long that is stretched an additional 1 mm exhibits 10% tensile strain.

In addition to tension and compression a material can undergo shear. Tension, compression, and shear are often referred to as the three modes of stress and strain. However, these three modes are not independent, as shown in **Figure 2**.

It has been established that the biologic response of tissues and cells depends strongly on the mode of the strain stimulus (tension, compression or shear), as well as on their magnitudes and temporal profiles ^{6, 7}. It is therefore of interest to determine which modes of strain and stress the tissues of the ONH are exposed to as IOP is elevated. Note that strains are generally not homogenous. When the LC deforms, some regions could be highly strained in different modes, while others remain largely unaffected. This is important because the biological effects on cells are likely to be strongly dependent on the local levels of strain or stress than on global levels.

We would also like to emphasize that mechanical stress, which represents forces, is not synonymous with notions of stress typically used in physiologic or metabolic contexts (e.g. ischemic or oxidative stress). Mechanical stress cannot be measured directly, and we believe it is strain that damages tissues. That said, stress is often used to predict the sites of and failure in engineering structures ¹ and has been correlated to damage in tissues ⁸, so it may be that while strain is causing the damage, stress is a better predictor of the sites of that damage ⁹.

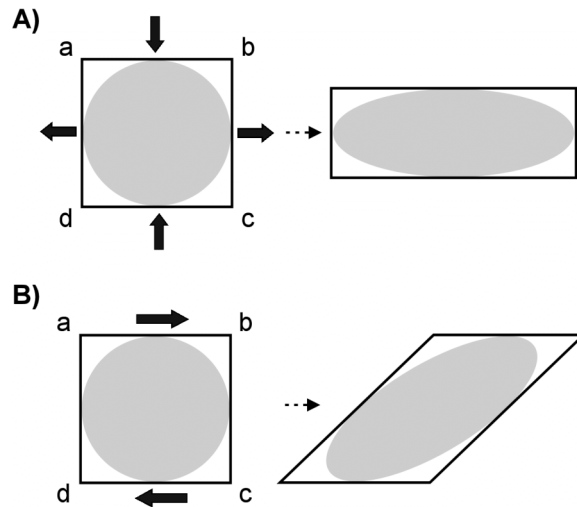


Figure 2. Schematic illustration of tissue straining in two dimensions. **A)** A square tissue region $abcd$ is deformed by forces that act normal to the faces of the square, represented by the black arrows. The tissue experiences tensile stretching in one direction and compression in another. Superimposed on the square tissue region is a circle that deforms with the tissue. **B)** The same tissue region is deformed by shearing forces that act tangential to the faces of the square. However, as this region deforms it does not only experience shear, but also extension and compression, as can be verified by noting how the distances between ac and bd change. In fact, the ellipses in the each panel are identical, showing that shearing is present in the deformation shown in the top row and elongation/compression is present in the deformation shown in the bottom row (Adapted from ¹⁰).

Stress and strain (*i.e.* forces and deformation) in a material are related to each other through material properties, and this constitutive relationship is intrinsic to each material. For a given load, a material that exhibits large strains is thought of as compliant. Conversely, a material that exhibits small strains for the same load is termed stiff. A stiff tissue such as sclera can have high stress but low strain, while an equal volume of compliant tissue, like retina, might have high strain even at low levels of stress. The simple description above does not account for many of the complexities in material properties that occur in soft biologic tissues, such as anisotropy, nonlinearity and viscoelasticity. These complexities are likely to be fundamental to understanding ocular mechanics and will be discussed in the context of scleral biomechanics below.

3- Scleral biomechanics

From a mechanical perspective, the eye is a pressure vessel, on which IOP produces deformation, strain, and stress. Through computational modeling, such as those presented in Section 4, the sclera has been shown to have a strong influence on how the LC deforms when IOP changes. Therefore, understanding the mechanical behavior of the sclera is essential to understanding IOP-induced LC deformations. One of the mechanisms by which scleral biomechanics can influence the response of the LC to IOP is illustrated in **Figure 3**.

Alas, describing the mechanical behavior of soft-tissue such as the sclera is a formidable undertaking that demands extensive experimental and mathematical efforts. The first step in characterizing scleral material properties is the development of an experimental mechanical test to measure the deformation of the tissue subjected to loads (e.g. uniaxial, biaxial, or pressurization tests). The second step is the development of a constitutive model (i.e. relationship between stresses and strains), which describes the tissue mechanical behavior as observed in the experiment and provides a mathematical representation of the tissue's material properties.

Historically, the sclera has been described as a thin-walled, spherical pressure vessel obeying the analytical equation known as Laplace's Law. Laplace's Law is useful to estimate the state of stress in non-biological pressure vessels, but it is inadequate for describing many aspects of the eye's mechanical response to variations in IOP. The sclera has been shown to exhibit several properties that violate the assumptions of Laplace's Law. First, the eye is a pressure vessel of non-uniform thickness¹¹⁻¹³. Second, in terms of its material properties, the sclera is nonlinear¹⁴⁻¹⁶, anisotropic^{16, 17}, and viscoelastic¹⁸⁻²⁰. These concepts are fundamental to understanding scleral and ONH biomechanics, and below we present them in greater detail.

Effects of Scleral Biomechanics on the ONH

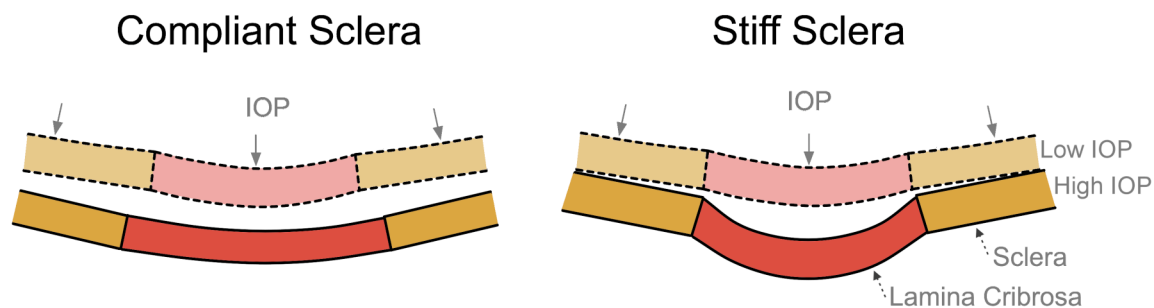


Figure 3. Influence of scleral mechanics on ONH mechanics. IOP induces large deformations on a compliant sclera (left), which are transmitted to the scleral canal, resulting in a large scleral canal expansion the pulls the LC taut despite the direct posterior force of IOP on the LC. Conversely, a stiff sclera deforms little under IOP (right), with small scleral canal expansions and little stretching of the LC, thus allowing the LC to be displaced posteriorly by the direct action of IOP on its anterior surface.

Nonlinearity is a property exhibited by most soft tissues, often as a consequence of collagen fibers within the tissue¹ (**Figure 4**). In a pressure vessel with linear material properties, the stiffness would remain constant during pressure-induced deformation,

whereas a nonlinear pressure vessel would experience either softening or stiffening as it deforms. Recent experiments have shown that the sclera exhibits a considerable increase in stiffness, at least five-fold, when exposed to an acute elevation of IOP from 5 to 45 mmHg¹⁵. This dramatic change shows the substantial impact that collagen fibers can have on scleral stiffness and deformation.

Anisotropy, as opposed to isotropy, is the property by which materials exhibit different stiffness in different directions. For thin biological tissues, anisotropy is primarily dictated by the organization of their fibrous structure, which is confined within the plane of the tissue, as illustrated in **Figure 4**. Unlike the cornea, scleral collagen fiber orientation has not been fully characterized. However, it has been shown through computational modeling that collagen fiber orientation and distribution are major determinants of scleral deformation²¹. Further experimental work is needed to better characterize scleral anisotropy and its effects on LC biomechanics.

Viscoelastic materials, such as the sclera, exhibit higher resistance to deformation when loaded quickly rather than slowly. Downs and co-workers characterized the viscoelastic material properties of normal rabbit and monkey peripapillary sclera^{18, 22} and found that the material properties of peripapillary sclera are highly time-dependent (viscoelastic). This behavior protects ocular tissues from large deformations during short-term spikes in IOP, which occur during blinks, eye rubbing, or high-speed impacts.

These three aspects of the sclera's material properties -nonlinearity, anisotropy and viscoelasticity- affect IOP-induced scleral deformations, but they are not the only important determinants of the eye's mechanical response. Material properties may be combined with thickness and shape to define another useful concept, that of structural, or effective, stiffness.

Studies of the scleral thickness of human^{13, 23} and monkey^{11, 12} eyes show that, on average, the human sclera is about twice as thick as the monkey sclera. The sclera is thinnest near the equator (as thin as 100 μm in both species), and thickest in the peripapillary region (average of 1000 μm in the human and 450 μm in the monkey). Large variations in peripapillary scleral thickness occur naturally and in pathologic conditions (e.g. myopia²⁴), and have been hypothesized to be an important determinant of individual susceptibility to IOP^{25, 26}. **Figure 5** illustrates how IOP-related stress is distributed in the peripapillary sclera in two situations: homogeneous thickness with a circular scleral canal, and inhomogeneous thickness with an elliptical scleral canal.

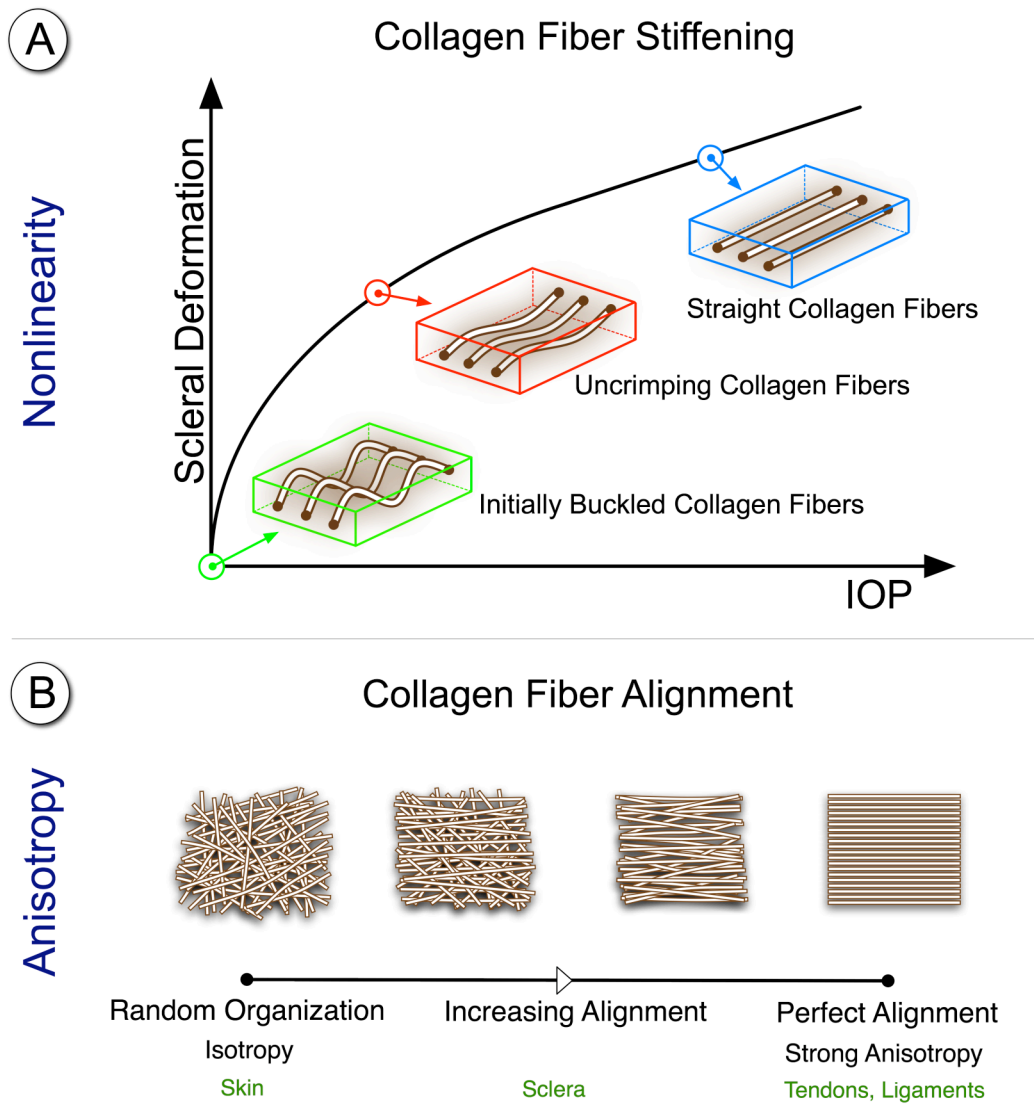


Figure 4. A) Nonlinearity is a property that sclera exhibits, in which the relationship between loading and deformation is not linear. At low IOP, collagen fibers are initially crimped, which makes the sclera more compliant. As IOP increases, the scleral collagen fibers uncrimp and eventually become straight, resulting in a dramatic increase in scleral stiffness, (an increase in the amount of IOP elevation necessary to produce the same deformation). **B)** Schematic illustration of the various degrees of planar anisotropy present in thin soft-tissues. Skin has a highly disorganized arrangement of collagen fibers and therefore resists loads similarly in many directions, a property known as isotropy. In contrast, tendons have well organized collagen fibers running principally in the longitudinal direction, and therefore these tissues sustain loads differently along and across their length, a property known as anisotropy. The sclera is thought to have a collagen fiber alignment that is between those of skin and ligaments.

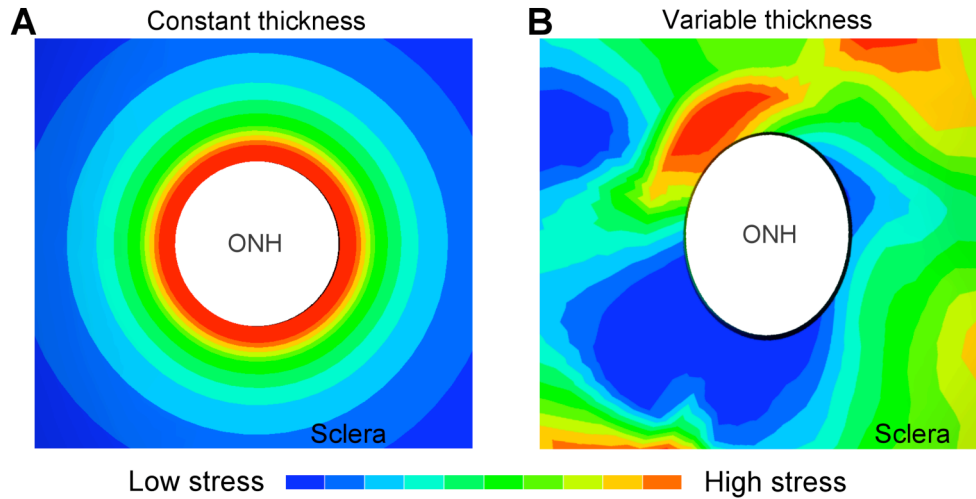


Figure 5. The thickness of the peripapillary sclera, and the size and shape of the scleral canal influence the magnitude and distribution of IOP-related stress within the peripapillary sclera, and within the ONH. Plots of stress within 3D biomechanical models of the posterior sclera and ONH illustrate how stress concentrates around the scleral canal. **A)** An idealized model with a circular canal and a perfectly spherical scleral shell wall of uniform thickness. **B)** An elliptical scleral canal with anatomic variations in scleral shell thickness. In both cases, the stresses concentrate around the canal, but the more realistic model shows stress that varies substantially around the canal and can extend further out into the sclera. For clarity, only the scleral tissues are shown.

4- ONH and LC biomechanics

4.1 Models of the ONH

Initial experimental studies of ONH biomechanics were often designed to examine and quantify a posterior deformation of the LC in response to an acute increase in IOP. Unfortunately, it is difficult to take measurements of the LC directly because it is fragile and relatively inaccessible, and therefore experimental efforts used one of two approaches: histological examination of ONH tissues fixed at different IOPs^{27, 28}; or measurement of acute deformations of the ONH surface through imaging, and using these deformations as a surrogate for the deformations of the underlying LC²⁹.

Both approaches produced interesting results. For example, histology-based studies found that acutely elevating IOP produced a posterior deformation of the LC (from 12 to 79 μm in humans^{27, 30}, and between 10 and 23 μm in monkeys³¹). However, these studies also highlighted the large variability in ONH geometry between individuals and the difficulties inherent in histomorphometry, which complicates distinguishing the effects of IOP from the natural differences between eyes. Imaging-based studies were subject to the assumption that IOP-induced deformations of the ONH surface are a good surrogate for deformations of the LC. Some experiments, as well as the modeling studies we describe below, have suggested that IOP-induced deformations of the ONH surface are not good predictors of LC deformations.

Recently, there have been advances in direct imaging of the acute deformations of the LC itself using second harmonic imaging³² or deep-scanning OCT³³ (**Figure 6**). Although promising, these technologies are still in development and have been unable to characterize the response of the ONH tissues to IOP.

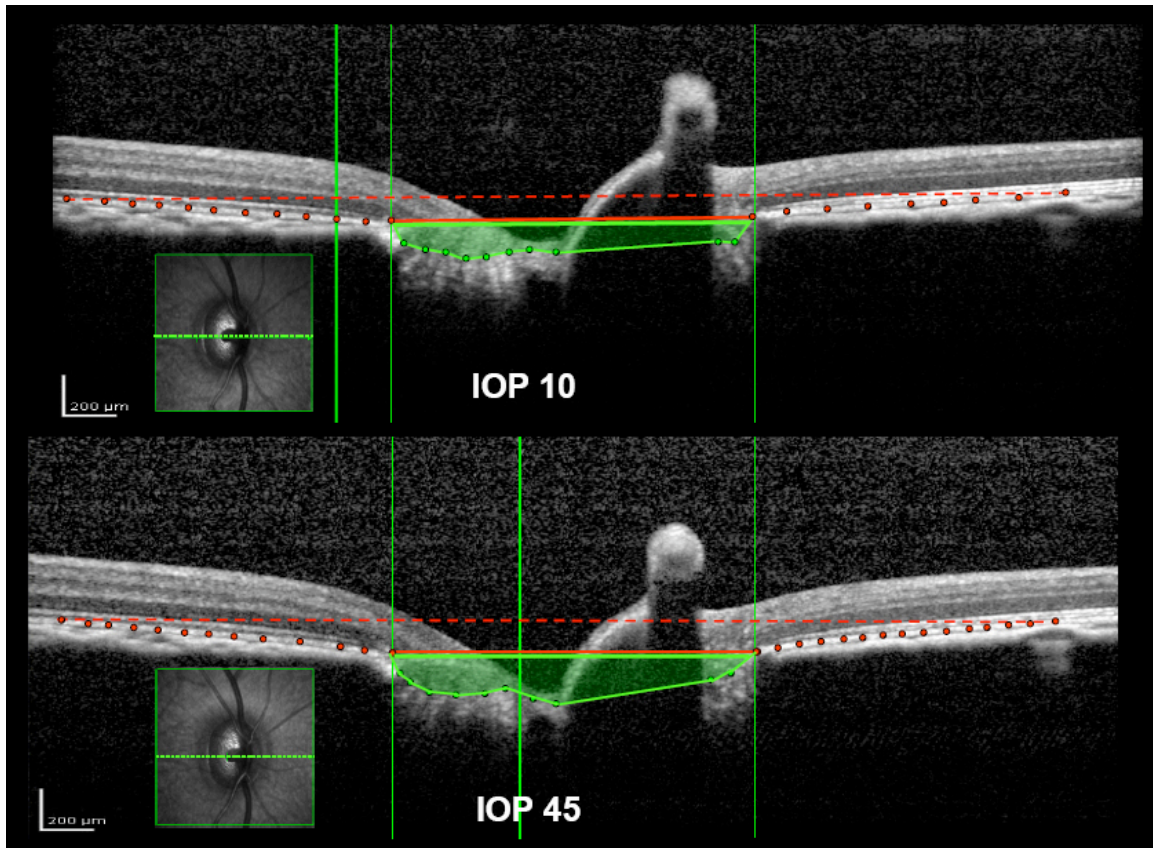


Figure 6. High Resolution Spectralis (Heidelberg Engineering, Heidelberg, Germany) Ocular Coherence Tomographic (OCT) B-Scans of a normal monkey eye obtained at 10 mmHg (top) and 45 mmHg (bottom) IOP. Bruch's membrane and the anterior LC surface have been delineated (red and green dots, respectively). The area enclosed by the anterior surface of the LC and a plane defined at Bruch's membrane (BM) opening (area shaded green) is larger in the scan at 45 mmHg. There was no detectable lateral expansion of the scleral canal (vertical green lines), suggesting that the increase in IOP produced posterior lamellar deformation. Using a second reference plane parallel to BM opening (dashed red lines), it is also visible that the BM is outwardly bowed at high IOP, which suggests that there is IOP-induced posterior deformation of the peripapillary sclera. While choroidal compression may contribute to this finding, we believe that the behavior of BM is principally related to the behavior of the sclera. The parameters computed from the images are volumetric, but are shown here in cross section for clarity.

In the absence of robust experimental methods for measuring the response of ONH tissues to acute IOP changes, several researchers have adopted a modeling approach to characterize the mechanical behavior of the ONH. Some of the models have been analytical^{34, 35}, but the majority are numerical^{36, 37}. While analytic approaches are attractive for their elegance, numerical models can incorporate more complex and realistic ONH geometry and material properties, such as the variable sclera thickness, anisotropy, and nonlinearity that were discussed in Section 3.

An early example of numerical modeling is the work of Bellezza *et al.*³⁶. They used a model to study the effects of the size and eccentricity of the scleral canal on the mechanical response of the ONH, and found that **IOP-related stresses within the connective tissues of the ONH could be substantial**, up to two orders of magnitude

larger than IOP, **even at low levels of IOP**. Models with larger canal diameters, more elliptical canal openings, and thinner sclera all showed increased stresses in the ONH and peripapillary sclera for a given IOP increase. Bellezza's models were highly idealized with a rudimentary description of the LC, but were the first to leverage the power of numerical models for the analysis of ONH biomechanics. Sander *et al.* developed the most advanced analytic models to date, and arrived at similar conclusions³⁴.

Sigal *et al.* developed a more comprehensive generic model to study ONH biomechanics³⁷ (**Figure 7**). Unlike the initial models by Bellezza *et al.*, these models incorporated a simplified central retinal vessel and pre- and post-laminar neural tissues, which allowed them to compare the simulated IOP-induced displacements and deformations of the ONH surface with those of the LC. The central retinal vessel had only a minimal effect on ONH biomechanics and was not included in later models. More importantly, they found that the IOP-induced deformations of the ONH surface and LC, while related, are somewhat decoupled, and therefore that the **displacements of the ONH surface might not be a good surrogate for those of the LC**. This result was later also obtained with more complex models with eye-specific geometry of the ONH (described below), and observed in recent experiments³³.

In a later study, Sigal *et al.*²⁶ parameterized various geometric and material details of their model, and varied them independently to assess their impact on a host of outcome measures, including changes in the shape of the ONH tissues (such as cup to disc ratio), and stress and strain within the LC and neural tissues. This work identified **the five most important determinants of ONH biomechanics (in rank order) as: the compliance of the sclera, the size of the eye, IOP, the compliance of the LC, and the thickness of the sclera**. Their study was the first to quantify the important role of scleral properties on ONH biomechanics that we have described above in Section 3. Parametric studies such as these are important because they can be used to identify the biomechanical factors that warrant more in-depth study, as well as those factors that are unlikely to have a significant influence, thus providing information useful for focusing future experimental efforts.

Parametric models have also been leveraged to quantify the strength of the interactions between the factors that affect ONH biomechanics, that is, how the level of one factor influences another³⁸. An example is represented by the concept of structural stiffness discussed above, where the mechanical response of the sclera depends on its thickness and on its material properties. Increasing the stiffness or thickness of the sclera independently lead to reduced deformations transmitted to the ONH. However, if the sclera is stiff, then its thickness has very little effect, or if the sclera is thick then its stiffness matters less. Identifying the strong interactions between factors is important because it facilitates interpretation of experiments that find, or fail to find, correlations between parameters and effects.

Notwithstanding their advantages over analytic models, the generic numeric models cannot, by design, make predictions of the biomechanics of a specific eye, and ultimately it is specific eyes for which we would like to predict the effects of IOP. To address this limitation eye-specific models have been developed based on 3D reconstructions of monkey³⁹⁻⁴¹ and human⁴² eyes, with a long term goal of building models based on clinical imaging of living eyes and use them in the determination of interventional target IOP.

Sigal and coworkers reconstructed eye-specific models of human eyes based on histological sections of donor tissue (**Figure 8**)⁴². These models were similar to their generic models in the sense that they incorporated load-bearing (sclera, LC and pia mater) as well as pre- and post-laminar neural tissues into the analyses. They used these models to study the relative influences of geometry and material properties on the response of the ONH to changes in IOP^{43, 44}. Their results were somewhat surprising in that the differences in geometry between individual ONHs had a more limited influence on ONH biomechanics than the properties of the surrounding sclera. They also found, consistent with the results obtained using generic models, that the IOP-induced deformations of the ONH surface are likely not a good surrogate for the deformations of the LC. Eye-specific models also show that as IOP increases the scleral canal expands, tautening the LC,, and that the magnitude of the compressive strains is higher than that of the tensile or shear strains¹⁰. Although it is now clear that the various modes of strain (tensile, compressive and shear) are related and all occur simultaneously within the ONH, their relative magnitudes in the models could have been a consequence of the assumed material properties. The models of Sigal *et al.* have some limitations: the reconstruction methods might not have removed all the artifacts that arise due to warping of the histological sections during preparation; and that since the models are reconstructed from donor human eyes, the studies were unable to test some hypotheses in the development of glaucoma.

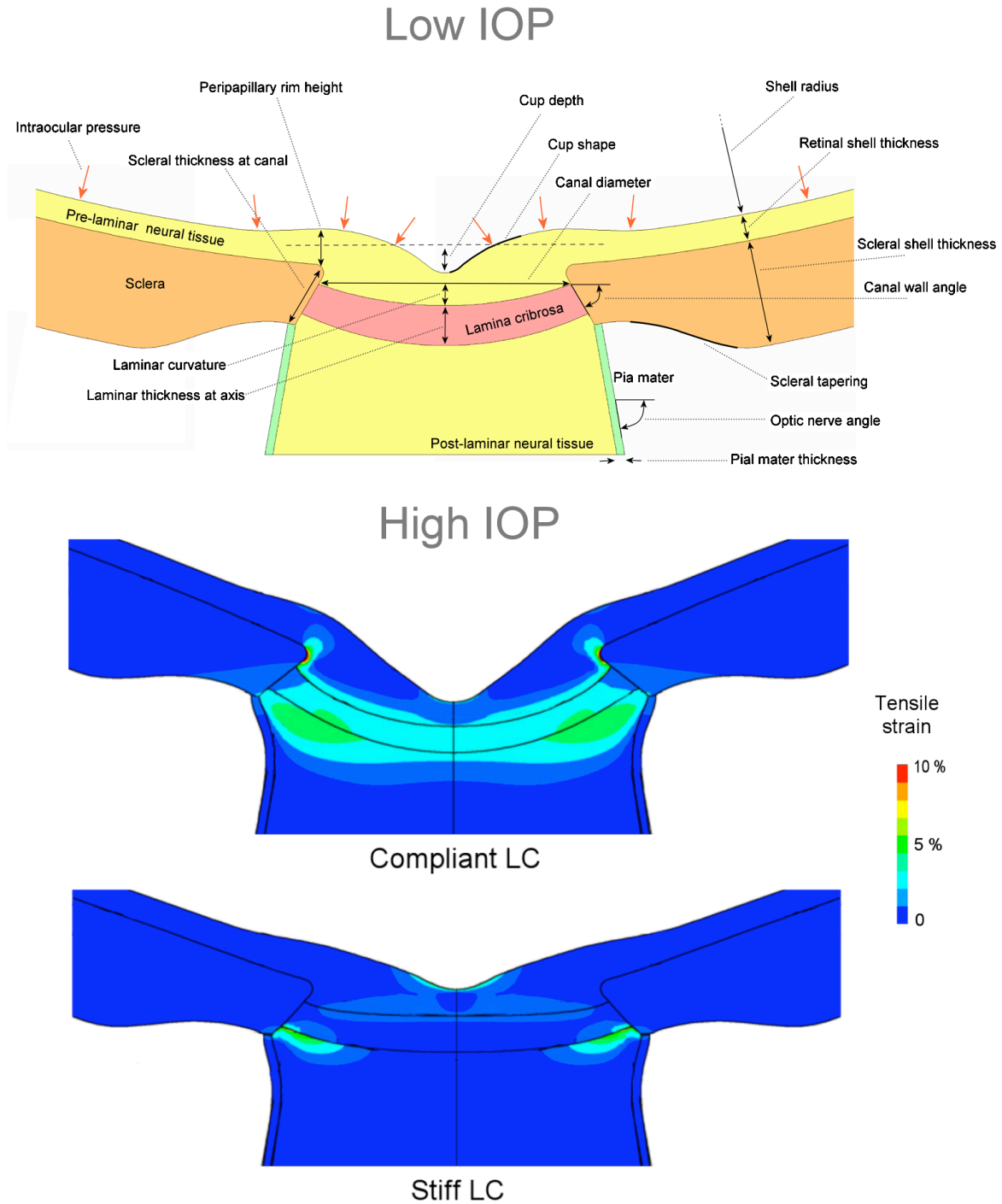


Figure 7. Generic models allow variation of parameters (top) to assess their independent, or combined, effects on ONH biomechanics; Contour levels of tensile strain computed for an increase in IOP of 25 mmHg for two models that only differ in lamellar stiffness (middle and bottom). For clarity the deformation of the loaded models has been exaggerated five times, and an outline of the undeformed geometry has been overlaid. A more compliant LC is subject to higher strain and larger posterior deformation.

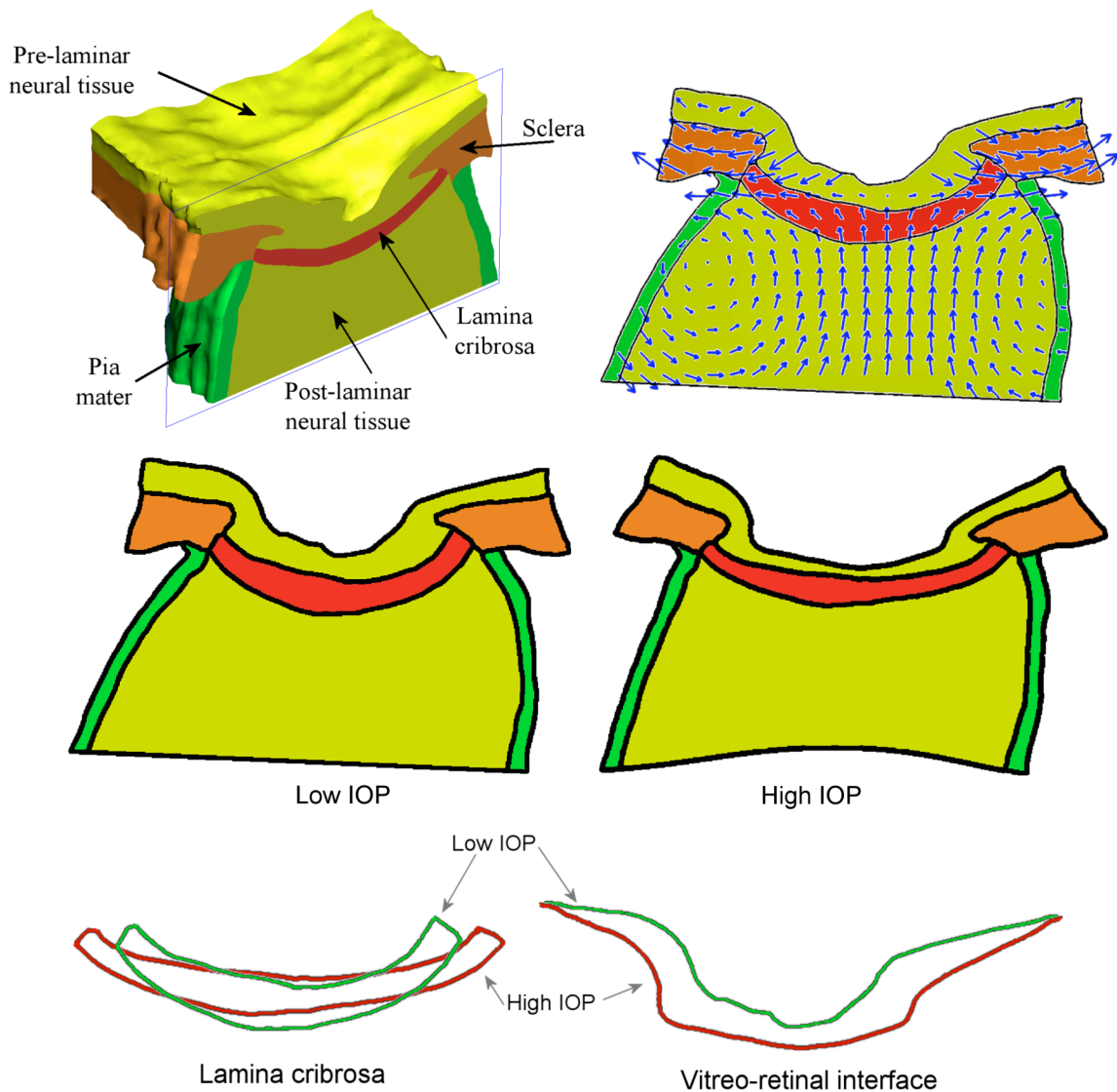


Figure 8. Eye-specific model reconstructed from an ostensibly healthy human donor eye simulated for an increase in IOP from 5 to 50 mmHg. The top left image is a 3D view of the model cut sagittally to show the interior. As IOP is increased the tissues deform. The displacement vectors are shown on the top right overlaid on a sagittal cross section. The vectors were computed in 3D, with their 2D projections shown. Vector lengths are proportional to the magnitude of the total displacement, with the scale exaggerated for clarity. The middle row shows the sagittal cross sections of the model at low (left) and high (right) IOP. Deformations are exaggerated fivefold for clarity. Visible are effects such as the rotation of the sclera, the flattening of the cup, the thinning of the LC and pre-laminar neural tissues and the anterior movement of the central regions of the optic nerve relative to the LC. To highlight the deformations of the LC and vitreo-retinal interface these are shown in the bottom row, with low (green) and high (red) IOP outlines overlaid. The outlines show the stretching of the LC in the plane of the sclera, and the deepening of the cup. Note that these simulations were carried out assuming incompressible materials, and therefore that the thinning of the LC and the pre-laminar neural region do not represent a reduction in tissue volume, only a redistribution.

4.2 Models of the LC

A different approach for eye-specific finite element modeling has been adopted by Downs, Roberts, and coworkers that focuses only on the collagenous load-bearing tissues of the sclera and lamina cribrosa. Using a microtome-based technique to compile consecutive episcopic images of a surface-stained, embedded tissue block face, they are able to reconstruct the details of the laminar microarchitecture in 3D at high resolution⁴⁵. The ability to gather data from contralateral normal and glaucomatous monkey eyes makes this approach especially powerful and has provided insight into tissue-level morphometric changes that occur in response to chronic IOP elevations³⁹⁻⁴¹.

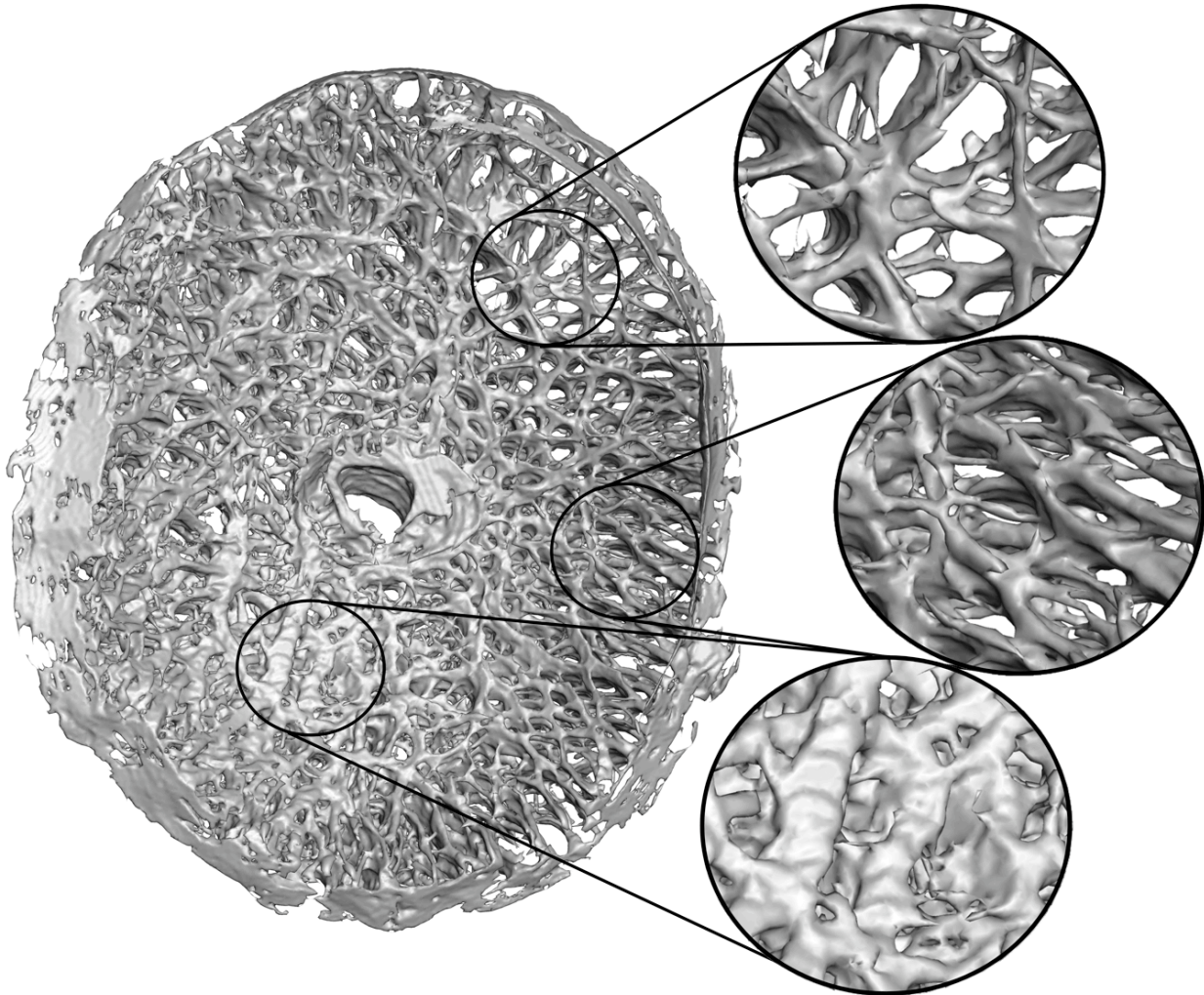


Figure 9. High resolution 3D reconstruction the lamina cribrosa from a monkey eye obtained using an episcopic serial imaging technique optimized for connective tissue detection. Note the regional variation in both connective tissue density and predominant laminar beam orientation throughout the lamina cribrosa. These spatial variations in microarchitecture will affect the regional deformation and load-bearing characteristics of the lamina cribrosa both as a whole and at the level of the individual laminar beams. This data has been used to develop finite element models describing both the macro- and beam-level mechanical environment in the ONH, such as those shown in Figure 10.

The first use of these reconstructions in the context of FE analysis has been to define descriptions of the LC that capture the inhomogeneity of the LC connective tissue structure (**Figure 9**). In these models, the regional variations in LC connective tissue volume fraction and predominant laminar beam orientation are analyzed in small regions, the “elements”, to define local material properties for the laminar regions of the model. Thus, regions within the LC with higher and lower porosity behave mechanically with greater and lesser compliance, respectively, and regions that exhibit strong directional orientation of laminar beams resist deformation more strongly, i.e. are stiffer, in those directions. This approach has demonstrated the importance of representing regional LC connective tissue inhomogeneity and anisotropy into models to capture the biomechanical behavior of the LC ⁴⁶. These models have also suggested that the LC may become more compliant in the early stage of glaucoma development despite an apparent increase in laminar connective tissue.

The continuum-level method described above homogenizes small elemental regions of LC microarchitecture into a bulk description of their effective material properties, precluding an analysis of the beam-level mechanical environment within the LC. To address this limitation, Downs and colleagues have developed a micro-scale modeling approach based on a substructuring paradigm. In this technique, continuum element-level displacement predictions from a parent model serve as inputs to corresponding element-sized micro-models so that resultant stresses and strains within laminar beams may be calculated (**Figure 10**). This technique reveals not only the complexity of IOP-related stresses and strains within the lamina cribrosa beams themselves, but also shows that beam-level stresses and strains are higher than those calculated using models that do not explicitly model the LC beams ⁴⁷. Furthermore, these micro-FE models predict that there are individual laminar beams with levels of IOP-related strain that are likely pathologic. While still in its early stages, this work holds the possibility of testing hypotheses about failure mechanisms and cellular responses at the level of the laminar beams.

In a complementary approach to the substructuring method described above, Kodiyalam and coworkers have developed a technique to analyze the entire LC using voxel-based FE models derived from the serial datasets described above ⁴⁸. These models are generated by directly converting image voxels into finite elements, and are analyzed using specialized algorithms optimized for the computational demands of this approach. Analysis of these voxel models is computationally intensive and requires massive storage and computer cluster resources to manage. Like the substructuring method, this approach explicitly represents the beams of the lamina cribrosa and therefore may be useful for characterizing the mechanical environment to which astrocytes are exposed. In its current implementation, these voxel models also account for a highly compliant neural tissue component within the porous LC space and may therefore provide insight into the effect of the translaminar pressure gradient on axoplasmic flow, and the tissues and cells of the ONH.

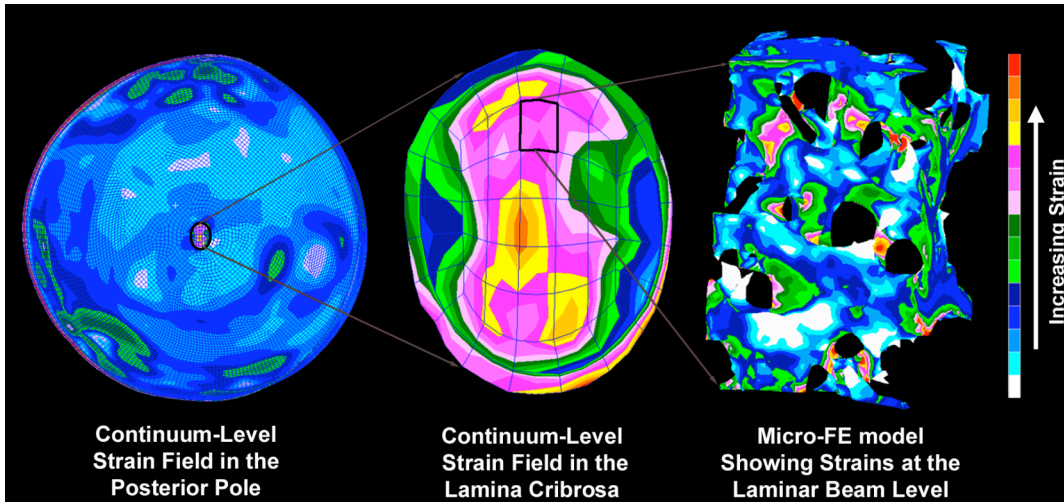


Figure 10. Multi-scale modeling of the mechanical environment of the lamina cribrosa. The image on the left shows the strain distribution within a continuum level model of the connective tissues of the posterior pole of the eye. Note that thickness variations in the sclera give rise to a non-uniform distribution of strain within the shell and that the strains are lower in the sclera than in the more compliant lamina cribrosa. The middle image shows a detail of the strain field within the continuum representation of the lamina cribrosa. While this portion of the FE model has been assigned regional material properties related to the amount and orientation of the lamellar beams (based on 3D reconstruction data such as that in Figure 9), the continuum description represents a bulk homogenization of the specific microarchitecture in each element. The right image shows the distribution of strains in a micro-model that captures the explicit lamellar beam microarchitecture associated with a particular element of the lamellar reconstruction. At this scale the strain distribution is complex.

Pathophysiology

4.3 Other measures of acute IOP-related changes in the ONH

ONH, retinal, and choroidal blood flow are also affected by acute IOP elevations. For example, studies using microspheres⁴⁹ have suggested that volume flow within the prelaminar and anterior lamellar capillary beds is diminished once ocular perfusion pressure (defined as the systolic arterial blood pressure plus 1/3 of the difference between systolic and diastolic pressures minus IOP) falls below 30 mm Hg.

While a direct link to mechanical strain has not been established, axonal transport is compromised in the LC at physiologic levels of IOP⁵⁰ and is further impaired following acute IOP elevations^{2,51}. In a biomechanical context, several explanations might account for these observations. First, as the LC pores change conformation due to IOP-related mechanical strain, slight constriction of the axon bundles within these pores may occur, directly hindering axoplasmic transport. Second, it may be that the IOP-related reduction in blood flow in the lamellar region impairs the mitochondrial metabolism that drives axoplasmic transport. Finally, axoplasmic transport could be sensitive to the magnitude of the translaminar pressure gradient, such that the active transport mechanisms within the bundles are required to overcome the resistance of the pressure gradient to drive axoplasmic flow.

In summary, while connective tissue dynamics should, by themselves, directly and indirectly influence astrocyte and glial metabolism and axonal transport, glaucomatous damage within the ONH may not necessarily occur at locations with the highest levels of IOP-related connective tissue strain or stress, but rather at those locations where the translaminar tissue pressure gradient is greatest and/or where the axons, blood supply, and astrocytes and glia have been made most vulnerable. Further studies are necessary to elucidate the link(s) between IOP, mechanical strain, blood flow, astrocyte and glial cell homeostasis, and axoplasmic transport in the ONH, in both the physiologic and diseased states.

4.4 Cellular mechanics

Laminar astrocytes have been shown to respond to changes in hydrostatic or barometric pressure⁵². However, the uncertain role of hypoxia and the lack of astrocyte basement membrane deformation in the barometric pressure model has led to questions concerning the true nature of the insult delivered to the cells in the hydrostatic pressure model. Instead, recent studies have concentrated on genomic and biochemical characterization of ONH astrocytes grown on membranes subjected to controlled levels of strain⁵³. *In vitro* techniques face the difficulty of subjecting the cells to the complex, multi-mode, 3D strain fields that exist within the ONH. Subjecting the cells to this environment while still being able to test their response is a major challenge for both biology and engineering. We expect that, in time, strain predictions from computational FE models and data on IOP fluctuation from telemetric IOP monitoring studies will allow these experiments to more closely model physiologic and pathophysiologic conditions in the normal and glaucomatous eye.

5 Restructuring and remodeling of the ONH

5.1 Normal aging

As demonstrated in the previous sections, the connective tissues of the ONH experience substantial levels of IOP-related stress and strain, even at physiologic levels of IOP. We propose that exposure to these levels of stress and strain over a lifetime result in a host of gradual changes to both connective tissues and vasculature that underlie the process of normal aging in the ONH. Thus the biological processes associated with glaucomatous damage and remodeling of ONH tissues occur in tandem with the normal physiologic remodeling processes associated with aging and it is therefore important to characterize the age related changes that occur in the ONH connective tissues.

At the cellular level, age-related changes in the ONH include increased collagen deposition in the lamellar ECM and thickening of associated astrocyte basement membranes^{54, 55}. Mechanically, it has also been shown that the lamina cribrosa and sclera become more rigid with age⁵⁴. All of these changes may act in concert with age-related decreases in volume flow within the lamellar capillary network to compromise nutrient diffusion across the lamellar ECM to the axonal bundles in older patients.

5.2 Alterations in connective tissue architecture, cellular activity, axoplasmic transport and blood flow in early glaucoma

Pathophysiologic levels of stress and strain can induce aberrant changes in cell synthesis and tissue composition and microarchitecture that exceed the effects of normal aging. Two important pathophysiologies can follow in glaucoma: 1) mechanical yield and/or failure of load-bearing connective tissues in the ONH, and 2) progressive damage of adjacent axons by multiple mechanisms (**Figure 1**). Importantly, changes that compromise the load-bearing function and alter the stress and strain environment within the ONH connective tissues may act in a mechanical feedback manner to further degrade the biomechanical and cellular milieu.

Early glaucomatous damage has not been rigorously studied in humans because of the paucity of well-characterized cadaveric eye specimens with early damage. Analysis of early experimental glaucoma in monkeys with moderate IOP elevations has revealed several aspects of the early changes in ONH and peripapillary scleral connective tissue architecture and material properties. These changes (**Figure 11**) include 1) thickening of prelaminar neural tissues⁴⁰; 2) enlargement and elongation of the neural canal³⁹; 3) posterior deformation and thickening of the lamina cribrosa with mild posterior deformation of the scleral flange and peripapillary sclera⁴¹; 4) hypercompliance of the LC in some animals³¹; and 5) alterations in the viscoelastic material properties of the peripapillary sclera^{18, 22}.

The effects of early glaucoma on cellular activity, axoplasmic transport, and blood flow have not been rigorously documented in the monkey model. In the rat eye, however, genomic techniques have been used to characterize changes in the genome of ONH tissues (within which a minimal lamina cribrosa exists in the rat) following exposure to experimentally elevated IOP⁵⁶. Within eyes that exhibited an early focal stage of orbital optic nerve axon loss an increase in gene expression was noted for several ECM components including tenascin C, fibulin 2, and the matrix metalloproteinase inhibitor TIMP-1, along with increased expression of genes governing the initiation of cell division. In a rat optic nerve transection model, differences in gene expression patterns

suggested that the focal axon loss mentioned above were due to IOP effects rather than simply axonal loss.

5.3 Alterations in connective tissue architecture, cellular activity, axoplasmic transport and blood flow in later stages of glaucomatous damage

The classic morphological description of glaucomatous damage – profound posterior lamellar deformation, excavation of the scleral canal beneath the optic disc margin, and compression of the LC – derives largely from human and monkey eyes with moderate, severe and end-stage glaucomatous damage^{57, 58}. These studies often encompass a broad range of glaucomatous damage to specimens which unfortunately have a poorly characterized IOP-history. Thus, a temporal narrative of the progression of events in the IOP-insulted ONH has not emerged. Nevertheless, histologic studies have reported several consistent phenomena occur in glaucomatous tissue including withdrawal of astrocyte processes from lamellar beams⁵⁹, astrocyte basement membrane disruption and thickening, degradation of elastin within the lamellar beams, physical disruption of the lamellar beams, and remodeling of the ECM.^{60, 61} It is reasonable to assume that many of these effects are due to IOP-induced alterations in the synthetic activities of resident cell populations.^{59, 62}

Alterations in axoplasmic transport at the lamina cribrosa⁶³ level has been described in human and monkey eyes exposed to chronic IOP elevation, along with a complicated array of ONH, retinal and choroidal blood flow alterations⁶⁴. However, because direct observation of ONH blood flow at the level of the peripapillary sclera and the LC capillaries level is not yet technically feasible, a rigorous study of the primary effect of IOP on blood flow remains elusive. Techniques to elucidate the relationships between ONH blood flow, ONH connective tissue integrity, ONH glial cell activity and RGC axonal transport within individual human and animal eyes are needed to unify our understanding of the multiple levels of interaction in this system.

One link between IOP-related strain in the ONH and concomitant cellular response may be found in the study of the spatial distribution of integrin types within the nerve head. Integrins are proteins that span the basement membranes of lamellar astrocytes and capillary endothelial cells to bind to ligands in the ECM, providing a direct interaction between the cell cytoskeleton and the substrate to which the cell is attached. As such, integrins are ideally suited to act as critical components within a mechanosensory system that transduces IOP- and blood flow-related changes in the ONH into subsequent cellular activity. Morrison has described the location and alteration of integrin subunits in normal and glaucomatous human and monkey eyes⁶⁵ and has proposed that they are an important link between LC deformation and damage, LC connective tissue remodeling, and LC astrocyte mediated axonal insult in glaucoma.

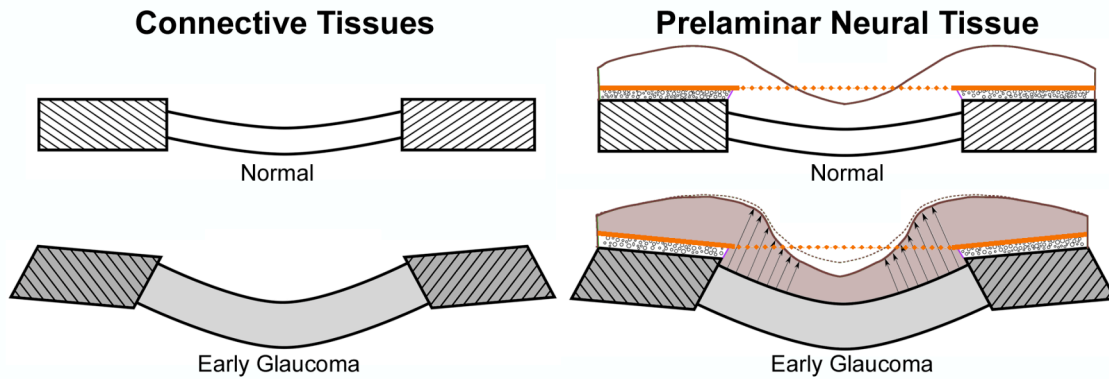


Figure 11. Remodeling and restructuring of the ONH in early experimental glaucoma. Sagittal section diagrams of the ONH, showing the peripapillary sclera (hatched) and the lamina cribrosa for normal and early glaucoma eyes. (Left) The early glaucoma eye has undergone permanent changes in ONH geometry including thickening of the lamina, posterior deformation of the lamina and peripapillary sclera, and posterior scleral canal expansion. (Right) Recent work has also shown that although the cup deepens relative to Bruch's membrane opening (dotted orange line) as can be detected by longitudinal confocal scanning laser tomography imaging (orange line) in early glaucoma, the prelaminar neural tissues (grey) are actually thickened rather than thinned. (Reprinted with permission from Hongli Yang).

Future directions

6.1 Clinical implications

There are currently no science-based tools to predict the level of IOP at which an individual ONH will be damaged. As described herein, computational modeling is a tool for predicting how a biological tissue with complex geometry and material properties will behave under varying levels of load. The goal of modeling eyes from human donors and monkeys with experimental glaucoma is to learn what aspects of neural, vascular and connective tissue architecture are most important to the ability of a given ONH to maintain structural integrity, nutritional and oxygen supply, and axoplasmic transport at physiologic and non-physiologic levels of IOP. In the future, clinical imaging of the ONH will seek to capture the architecture of these structures so as to allow clinically-derived biomechanical models of individual patient risk. Eventually knowledge of the relationship between IOP, mechanical strain, systemic blood pressure, and the resultant astrocyte and axonal mitochondrial oxygen levels will drive the clinical assessment of safe target IOP. Clinical characterization of the actual IOP insult through telemetric IOP monitoring will eventually allow better-controlled studies of individual ONH susceptibility. Finally, these modeling-driven targets for clinical imaging of subsurface structures will likely allow early detection of LC deformation and thickening. Once clinically detectable, early stabilization, and perhaps reversal, of these changes will become a new end point for target IOP lowering in most ocular hypertensive and all progressing eyes.

6.2 Basic research directions

From an engineering standpoint, large challenges remain to achieve basic and clinical knowledge regarding: 1) the mechanisms and distributions of IOP-related yield and failure in the lamellar beams and peripapillary sclera; 2) the mechanobiology of the astrocytes, glia, scleral fibroblasts, and LC cells; 3) the mechanobiology of axoplasmic flow within the LC; 4) the fluid dynamics governing the volume of blood flow within the lamellar capillaries and scleral and lamellar branches of the posterior ciliary arteries; and 5) nutrient diffusion to the astrocytes in young and aged eyes. We predict that knowledge gained from these studies will importantly contribute to new therapeutic interventions aimed at the ONH and peripapillary sclera of glaucomatous eyes.

1. Ethier CR, Simmons CA. *Introductory Biomechanics: From Cells to Organisms*, 1 ed. New York: Cambridge University Press, 2007.
2. Minckler DS, Bunt AH, Johanson GW. Orthograde and retrograde axoplasmic transport during acute ocular hypertension in the monkey. *Invest Ophthalmol Vis Sci* 1977;16:426-41.
3. Kendell KR, Quigley HA, Kerrigan LA, Pease ME, Quigley EN. Primary open-angle glaucoma is not associated with photoreceptor loss. *Invest Ophthalmol Vis Sci* 1995;36:200-5.
4. Panda S, Jonas JB. Decreased photoreceptor count in human eyes with secondary angle-closure glaucoma. *Invest Ophthalmol Vis Sci* 1992;33:2532-6.
5. Yucel YH, Zhang Q, Weinreb RN, Kaufman PL, Gupta N. Effects of retinal ganglion cell loss on magno-, parvo-, koniocellular pathways in the lateral geniculate nucleus and visual cortex in glaucoma. *Prog Retin Eye Res* 2003;22:465-81.
6. Edwards ME, Wang SS, Good TA. Role of viscoelastic properties of differentiated SH-SY5Y human neuroblastoma cells in cyclic shear stress injury. *Biotechnol Prog* 2001;17:760-7.
7. LaPlaca MC, Cullen DK, McLoughlin JJ, Cargill RS, 2nd. High rate shear strain of three-dimensional neural cell cultures: a new in vitro traumatic brain injury model. *J Biomech* 2005;38:1093-105.
8. Vorp DA, Schiro BJ, Ehrlich MP, Juvonen TS, Ergin MA, Griffith BP. Effect of aneurysm on the tensile strength and biomechanical behavior of the ascending thoracic aorta. *Ann Thorac Surg* 2003;75:1210-4.
9. Humphrey JD. Stress, strain, and mechanotransduction in cells. *J Biomech Eng* 2001;123:638-41.
10. Sigal IA, Flanagan JG, Tertinegg I, Ethier CR. Predicted extension, compression and shearing of optic nerve head tissues. *Exp Eye Res* 2007;85:312-22.
11. Downs JC, Blidner RA, Bellezza AJ, Thompson HW, Hart RT, Burgoyne CF. Peripapillary scleral thickness in perfusion-fixed normal monkey eyes. *Invest Ophthalmol Vis Sci* 2002;43:2229-35.
12. Downs JC, Ensor ME, Bellezza AJ, Thompson HW, Hart RT, Burgoyne CF. Posterior Scleral Thickness in Perfusion-Fixed Normal and Early-Glaucoma Monkey Eyes. *Invest Ophthalmol Vis Sci* 2001;42:3202-3208.
13. Olsen TW, Aaberg SY, Geroski DH, Edelhauser HF. Human sclera: thickness and surface area. *Am J Ophthalmol* 1998;125:237-41.
14. Woo SL, Kobayashi AS, Schlegel WA, Lawrence C. Nonlinear material properties of intact cornea and sclera. *Exp Eye Res* 1972;14:29-39.
15. Girard MJA, Downs JC, Bottlang M, Burgoyne CF, Suh JKF. An Anisotropic Hyperelastic Constitutive Model for Ocular Soft-Tissues, Part II - Application to Monkey Posterior Sclera. *Journal of Biomechanical Engineering* 2008;submitted. 19 pages. 7 figures. 3 tables.
16. Girard MJA, Downs JC, Bottlang M, Burgoyne CF, Suh JKF. Experimental Surface Strain Mapping of Porcine Peripapillary Sclera Due to Elevations of Intraocular Pressure. *Journal of Biomechanical Engineering* 2008;accepted. 14 pages. 7 figures.
17. Rada JA, Shelton S, Norton TT. The sclera and myopia. *Exp Eye Res* 2006;82:185-200.
18. Downs JC, Suh JK, Thomas KA, Bellezza AJ, Hart RT, Burgoyne CF. Viscoelastic material properties of the peripapillary sclera in normal and early-glaucoma monkey eyes. *Invest Ophthalmol Vis Sci* 2005;46:540-6.
19. Girard M, Suh JK, Hart RT, Burgoyne CF, Downs JC. Effects of storage time on the mechanical properties of rabbit peripapillary sclera after enucleation. *Curr Eye Res* 2007;32:465-70.

20. Siegwart JT Jr, Norton TT. Regulation of the mechanical properties of tree shrew sclera by the visual environment. *Vision Res* 1999;39:387-407.
21. Girard MJA, Downs JC, Bottlang M, Burgoyne CF, Suh JKF. An Anisotropic Hyperelastic Constitutive Model for Ocular Soft-Tissues, Part I - Theory. *Journal of Biomechanical Engineering* 2008;submitted. 21 pages. 7 figures. .
22. Downs JC, Suh JK, Thomas KA, Bellezza AJ, Burgoyne CF, Hart RT. Viscoelastic characterization of peripapillary sclera: material properties by quadrant in rabbit and monkey eyes. *J Biomech Eng* 2003;125:124-31.
23. Rausch SMK, Sigal IA, Norman RE, et al. Measurement of Scleral Thickness Distribution of Human Eyes Using Micro-MRI. E-Abstract 3306. Ft. Lauderdale FL USA: ARVO, 2007.
24. McBrien NA, Cornell LM, Gentle A. Structural and ultrastructural changes to the sclera in a mammalian model of high myopia. *Invest Ophthalmol Vis Sci* 2001;42:2179-87.
25. Burgoyne CF, Downs JC, Bellezza AJ, Suh JK, Hart RT. The optic nerve head as a biomechanical structure: a new paradigm for understanding the role of IOP-related stress and strain in the pathophysiology of glaucomatous optic nerve head damage. *Prog Retin Eye Res* 2005;24:39-73.
26. Sigal IA, Flanagan JG, Ethier CR. Factors influencing optic nerve head biomechanics. *Invest Ophthalmol Vis Sci* 2005;46:4189-99.
27. Yan DB, Coloma FM, Metheetraitur A, Trope GE, Heathcote JG, Ethier CR. Deformation of the lamina cribrosa by elevated intraocular pressure. *Br J Ophthalmol* 1994;78:643-8.
28. Bellezza AJ, Rintalan CJ, Thompson HW, Downs JC, Hart RT, Burgoyne CF. Anterior scleral canal geometry in pressurised (IOP 10) and non-pressurised (IOP 0) normal monkey eyes. *Br J Ophthalmol* 2003;87:1284-90.
29. Meredith SP, Swift L, Eke T, Broadway DC. The acute morphologic changes that occur at the optic nerve head induced by medical reduction of intraocular pressure. *J Glaucoma* 2007;16:556-61.
30. Levy NS, Crapps EE. Displacement of optic nerve head in response to short-term intraocular pressure elevation in human eyes. *Arch Ophthalmol* 1984;102:782-6.
31. Bellezza AJ, Rintalan CJ, Thompson HW, Downs JC, Hart RT, Burgoyne CF. Deformation of the lamina cribrosa and anterior scleral canal wall in early experimental glaucoma. *Invest Ophthalmol Vis Sci* 2003;44:623-37.
32. Brown DJ, Morishige N, Neekhra A, Minckler DS, Jester JV. Application of second harmonic imaging microscopy to assess structural changes in optic nerve head structure ex vivo. *J Biomed Opt* 2007;12:024029.
33. Burgoyne CF, Williams G, Fortune B. Posterior Bowing of the Lamina Cribrosa and Peripapillary Sclera Are Clinically Detectable Within Heidelberg Spectralis 3D OCT Volumes of the Non-Human Primate (NHP) Optic Nerve Head (ONH) Following Acute and Chronic IOP Elevation. Program#/Poster# 3655/D1046. Ft. Lauderdale FL USA: ARVO, 2008.
34. Sander EA, Downs JC, Hart RT, Burgoyne CF, Nauman EA. A cellular solid model of the lamina cribrosa: mechanical dependence on morphology. *J Biomech Eng* 2006;128:879-89.
35. Edwards ME, Good TA. Use of a mathematical model to estimate stress and strain during elevated pressure induced lamina cribrosa deformation. *Curr Eye Res* 2001;23:215-25.
36. Bellezza AJ, Hart RT, Burgoyne CF. The optic nerve head as a biomechanical structure: initial finite element modeling. *Invest Ophthalmol Vis Sci* 2000;41:2991-3000.

37. Sigal IA, Flanagan JG, Tertinegg I, Ethier CR. Finite element modeling of optic nerve head biomechanics. *Invest Ophthalmol Vis Sci* 2004;45:4378-87.
38. Sigal IA, Flanagan JG, Ethier CR. Interactions between factors influencing optic nerve head biomechanics. Presented at the ASME 2007 Summer Bioengineering Conference. Keystone, Colorado: ASME, 2007.
39. Downs JC, Yang H, Girkin C, et al. Three Dimensional Histomorphometry of the Normal and Early Glaucomatous Monkey Optic Nerve Head: Neural Canal and Subarachnoid Space Architecture. *Invest Ophthalmol Vis Sci* 2007;48:3195-3208.
40. Yang H, Downs JC, Bellezza AJ, Thompson H, Burgoyne CF. 3-D Histomorphometry of the Normal and Early Glaucomatous Monkey Optic Nerve Head: Prelaminar Neural Tissues and Cupping. *Invest Ophthalmol Vis Sci* 2007;48:5068-84.
41. Yang H, Downs JC, Girkin C, et al. 3-D Histomorphometry of the Normal and Early Glaucomatous Monkey Optic Nerve Head: Lamina Cribrosa and Peripapillary Scleral Position and Thickness. *Invest Ophthalmol Vis Sci* 2007;48:4597-607.
42. Sigal IA, Flanagan JG, Tertinegg I, Ethier CR. Reconstruction of human optic nerve heads for finite element modeling. *Technol Health Care* 2005;13:313-29.
43. Sigal IA, Flanagan JG, Tertinegg I, Ethier CR. Modeling individual-specific human optic nerve head biomechanics. Part I: IOP-induced deformations and influence of geometry. *Biomech Model Mechanobiol* 2008.
44. Sigal IA, Flanagan JG, Tertinegg I, Ethier CR. Modeling individual-specific human optic nerve head biomechanics. Part II: influence of material properties. *Biomech Model Mechanobiol* 2008.
45. Burgoyne CF, Downs JC, Bellezza AJ, Hart RT. Three-dimensional reconstruction of normal and early glaucoma monkey optic nerve head connective tissues. *Invest Ophthalmol Vis Sci* 2004;45:4388-99.
46. Roberts MD, Burgoyne CF, Hart RT, Downs JC. Continuum-Level Finite Element Modeling of the Optic Nerve Head: Influence of Microstructure on Biomechanics in Normal and Early Glaucoma Eyes. *Invest Ophthalmol Vis Sci*, 2007.
47. Downs J, Roberts MD, Burgoyne CF, Hart RT. Finite Element Modeling of the Lamina Cribrosa Microstructure in Normal and Early Glaucoma Monkey Eyes. Presented at ARVO 2007. Ft. Lauderdale, FL, 2007:E-abstract 3301.
48. Kodiyalam S, Hart RT, Burgoyne CF, Roberts MD, Grimm J, Downs JC. Large-Scale Parallel Finite Element Simulations of Neural and Support Tissue in a Normal Monkey Lamina. Presented at ARVO 2007. Ft. Lauderdale Florida, 2007.
49. Geijer C, Bill A. Effects of raised intraocular pressure on retinal, prelaminar, laminar, and retrolaminar optic nerve blood flow in monkeys. *Invest Ophthalmol Vis Sci* 1979;18:1030-42.
50. Minckler D. Correlations between anatomic features and axonal transport in primate optic nerve head. *Tr. Am. Ophth. Soc.* vol. LXXXIV 1986:429-451.
51. Quigley HA, Anderson DR. Distribution of axonal transport blockade by acute intraocular pressure elevation in the primate optic nerve head. *Invest Ophthalmol Vis Sci* 1977;16:640-4.
52. Yang JL, Neufeld AH, Zorn MB, Hernandez MR. Collagen type I mRNA levels in cultured human lamina cribrosa cells: effects of elevated hydrostatic pressure. *Exp Eye Res* 1993;56:567-74.
53. Kirwan RP, Fenerty CH, Crean J, Wordinger RJ, Clark AF, O'Brien CJ. Influence of cyclical mechanical strain on extracellular matrix gene expression in human lamina cribrosa cells in vitro. *Mol Vis* 2005;11:798-810.
54. Albon J, Karwatowski WS, Easty DL, Sims TJ, Duance VC. Age related changes in the non-collagenous components of the extracellular matrix of the human lamina cribrosa. *Br J Ophthalmol* 2000;84:311-7.

55. Morrison JC, Jerdan JA, Dorman ME, Quigley HA. Structural proteins of the neonatal and adult lamina cribrosa. *Arch Ophthalmol* 1989;107:1220-4.
56. Johnson EC, Jia L, Cepurna WO, Doser TA, Morrison JC. Global Changes in Optic Nerve Head Gene Expression after Exposure to Elevated Intraocular Pressure in a Rat Glaucoma Model. *Invest Ophthalmol Vis Sci* 2007;48:3161-3177.
57. Emery JM, Landis D, Paton D, Boniuk M, Craig JM. The lamina cribrosa in normal and glaucomatous human eyes. *Trans Am Acad Ophthalmol Otolaryngol* 1974;78:OP290-7.
58. Quigley HA, Hohman RM, Addicks EM, Massof RW, Green WR. Morphologic changes in the lamina cribrosa correlated with neural loss in open-angle glaucoma. *Am J Ophthalmol* 1983;95:673-91.
59. Hernandez MR. The optic nerve head in glaucoma: role of astrocytes in tissue remodeling. *Prog Retin Eye Res* 2000;19:297-321.
60. Quigley HA, Dorman-Pease ME, Brown AE. Quantitative study of collagen and elastin of the optic nerve head and sclera in human and experimental monkey glaucoma. *Curr Eye Res* 1991;10:877-88.
61. Hernandez MR, Andrzejewska WM, Neufeld AH. Changes in the extracellular matrix of the human optic nerve head in primary open-angle glaucoma. *Am J Ophthalmol* 1990;109:180-8.
62. Clark AF, Browder SL, Steely HT, Wilson K, Cantu-Crouch D, McCartney MD. Cell biology of the human lamina cribrosa. Chapter 5. In: Drance SM, Anderson, D.R., editor. *Optic Nerve in Glaucoma*. Amsterdam/New York: Kugler Publications, 1995:79-105.
63. Quigley HA, Addicks EM. Chronic experimental glaucoma in primates. II. Effect of extended intraocular pressure elevation on optic nerve head and axonal transport. *Invest Ophthalmol Vis Sci* 1980;19:137-52.
64. Grunwald JE, Riva CE, Stone RA, Keates EU, Petrig BL. Retinal autoregulation in open-angle glaucoma. *Ophthalmology* 1984;91:1690-4.
65. Morrison JC. Integrins in the optic nerve head: potential roles in glaucomatous optic neuropathy (an American Ophthalmological Society thesis). *Trans Am Ophthalmol Soc* 2006;104:453-77.